Substrate-Free Multilayer Graphene Electronic Skin for Intelligent Diagnosis

Yancong Qiao[1#], Xiaoshi Li[1#], Jinming Jian[1], Qi Wu[1], Yuhong Wei[1], Hua Shuai[2], Thomas Hirtz[1], Yao Zhi[1], Ge Deng[1], Yunfan Wang[3], Guangyang Gou[1], Jiandong Xu[1], Tianrui Cui[1], He Tian[1*], Yi Yang[1*], and Tian-Ling Ren[1*]

[1]Institute of Microelectronics and Beijing National Research Center for Information Science and Technology (BNRist), Tsinghua University, Beijing, 100084, China
[2]Department of Physics, Engineering Physics,191 West Woodruff Avenue, The Ohio State University, Columbus, Ohio 43210
[3]Institute of Electronics, Tsinghua University, Beijing 100084, China

[#]These authors contributed equally to this work.
Email: rentl@tsinghua.edu.cn; yiyang@tsinghua.edu.cn; tianhe88@tsinghua.edu.cn

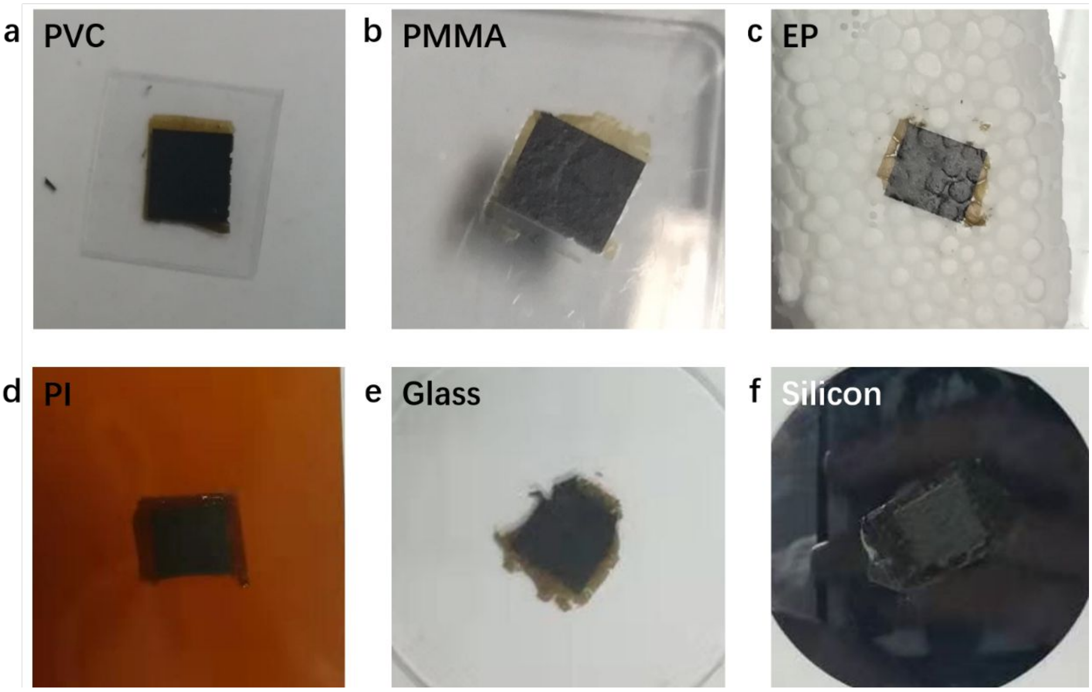

Fig. S1. SFG (1cm*1cm) transferred to (a) PVC, (b) PMMA, (c) EP, (d) PI, (e) glass, and (f) silicon.

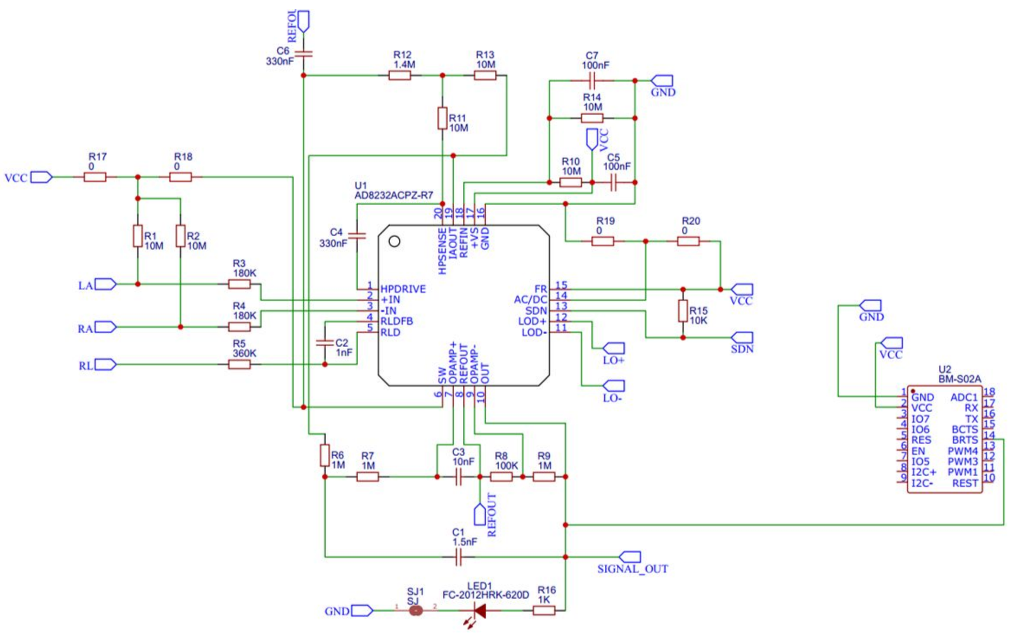

Fig. S2. The circuit diagrams. U1 is AD8232 and U2 is a Bluetooth module based on CC2540 (RF-BM-S02, SHENZHEN RFSTAR TECHNOLOGY CO., LTD.).

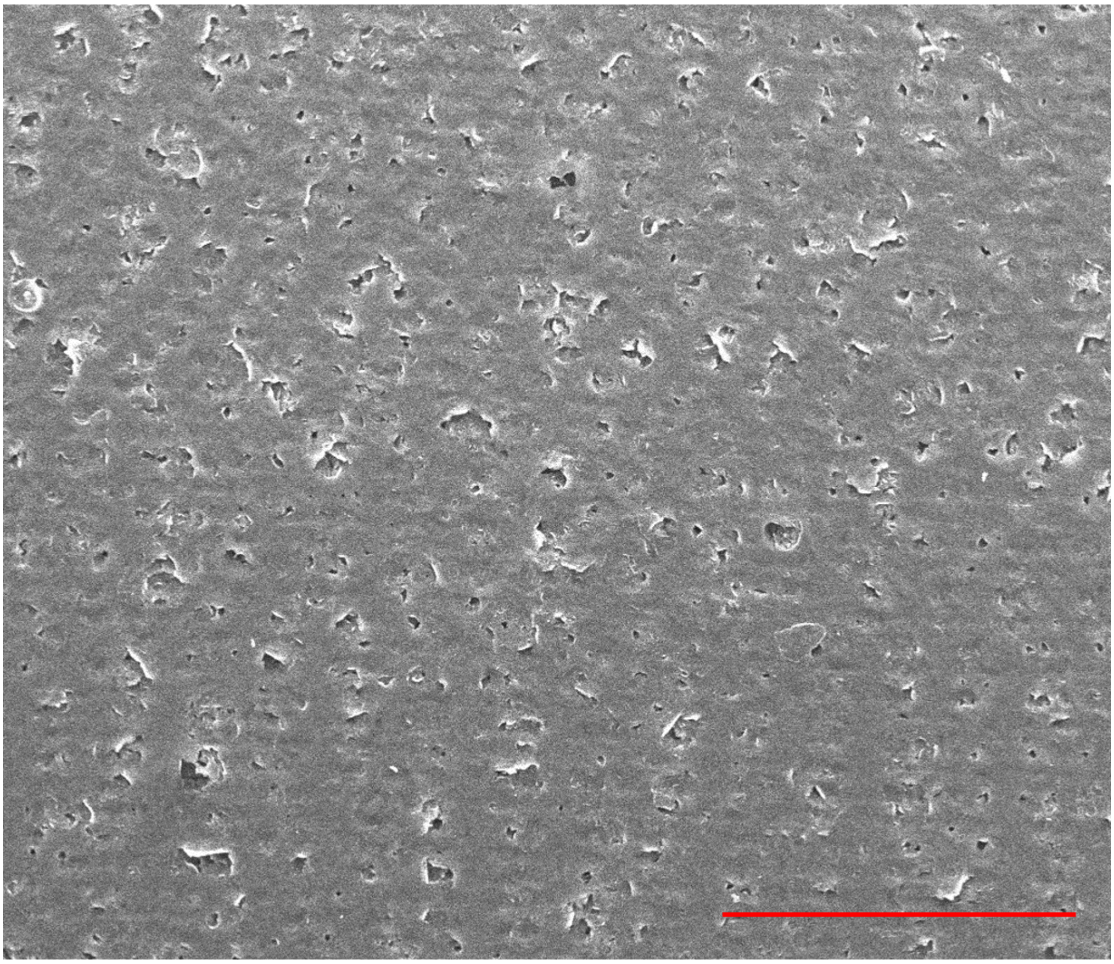

Fig. S3. The SEM image of the LSG with holes. Scale bar represents 1 mm. The size of holes is about 10 μm to 50 μm.

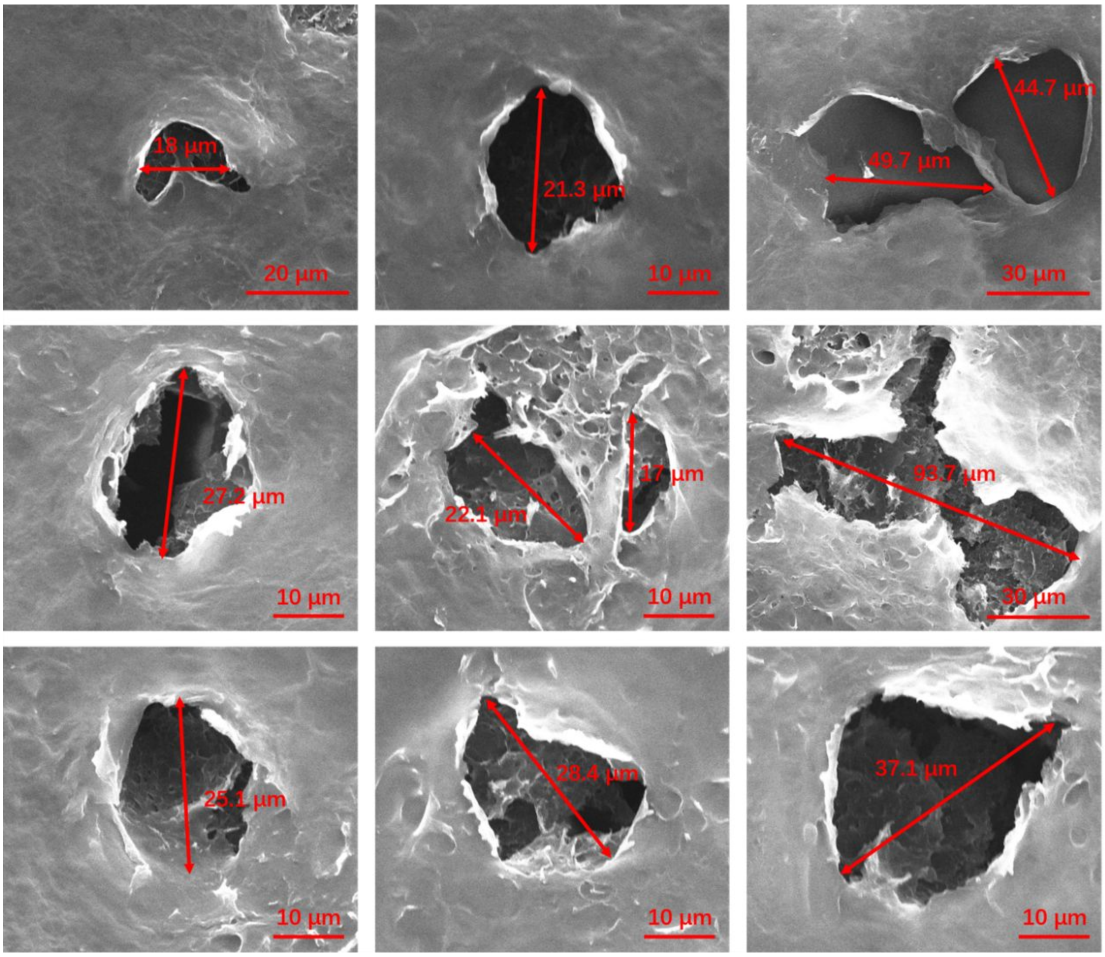

Fig. S4. The SEM image of the LSG with different holes. The size of holes is about 10 μm to 100 μm.

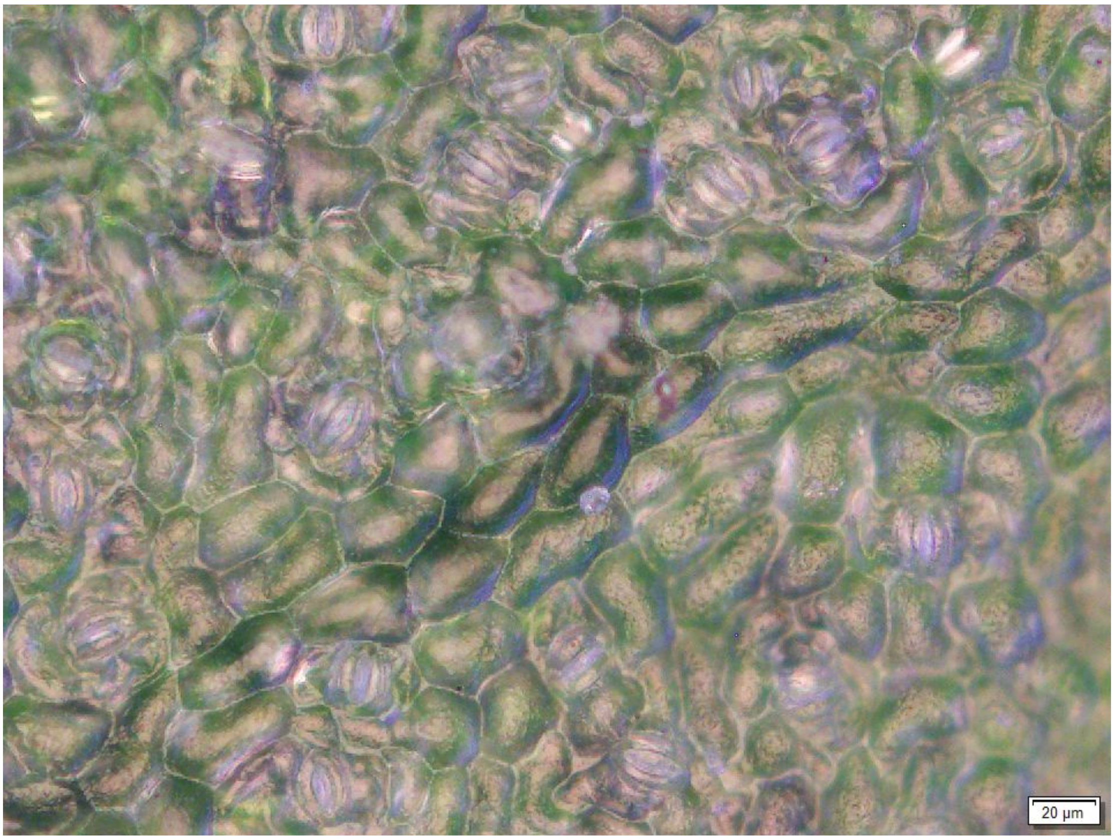

Fig. S5. The optical micrograph of the stomas on Hibiscus leaf.

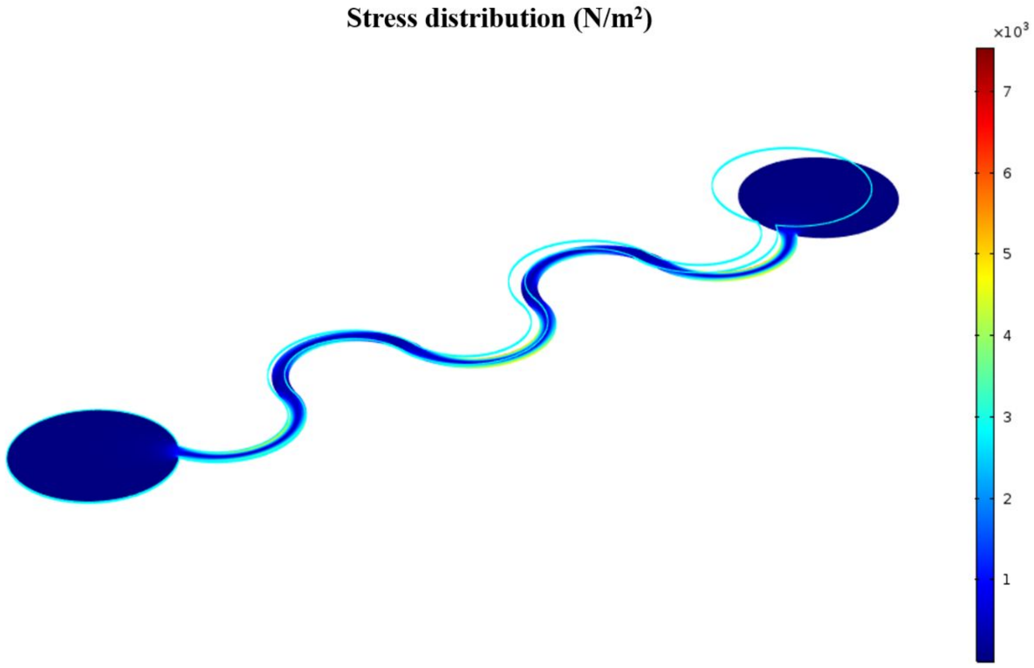

Fig. S6. The stress distribution of stress force distribution of the serpentine LSG simulated by COMSOL. The solid mechanics model is used to study the stress deformation and stress concentration point under steady state. The steady-state equation is $0 = \nabla S + Fv$. The left stress point is fixed constraint and the right boundary load is 1000 N/m^2. the simulation results show that the stress concentration is mainly concentrated at the maximum bending point of serpentine.

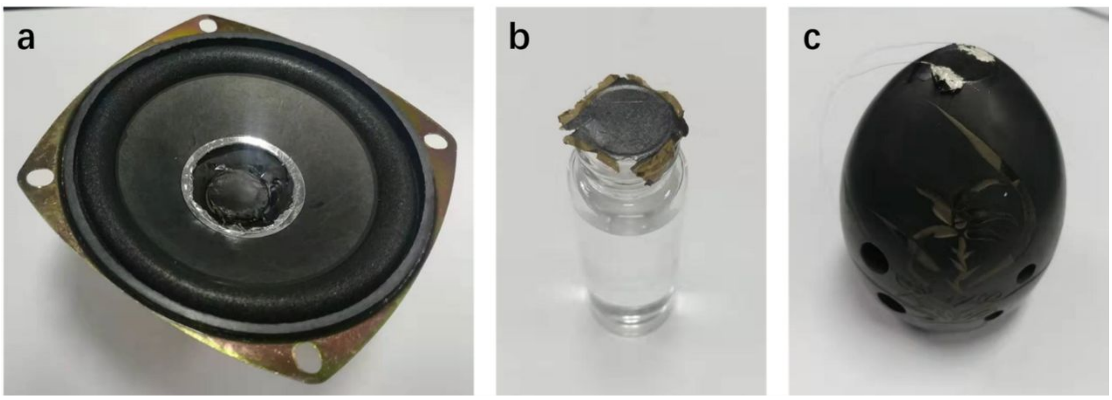

Fig. S7. The suspended SFG on the cavity of (a) loudspeaker, (b) bottle, and (c) Xun.

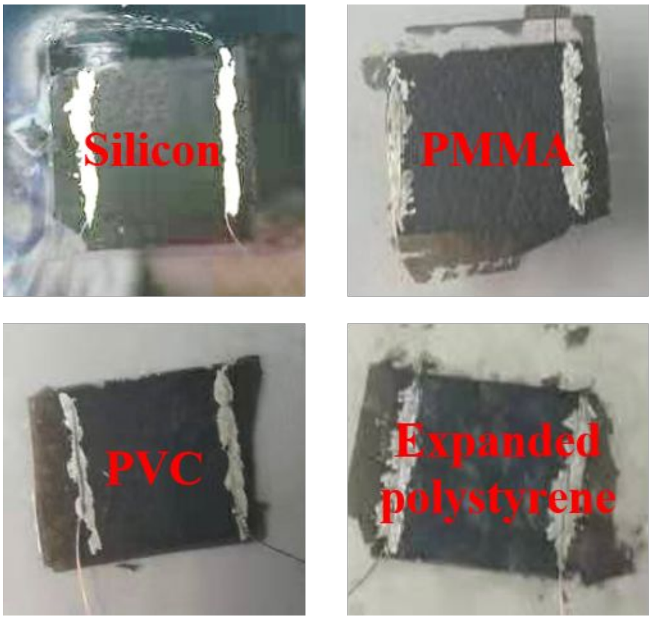

Fig. S8. The LSG transferred to different substrate as sound source.

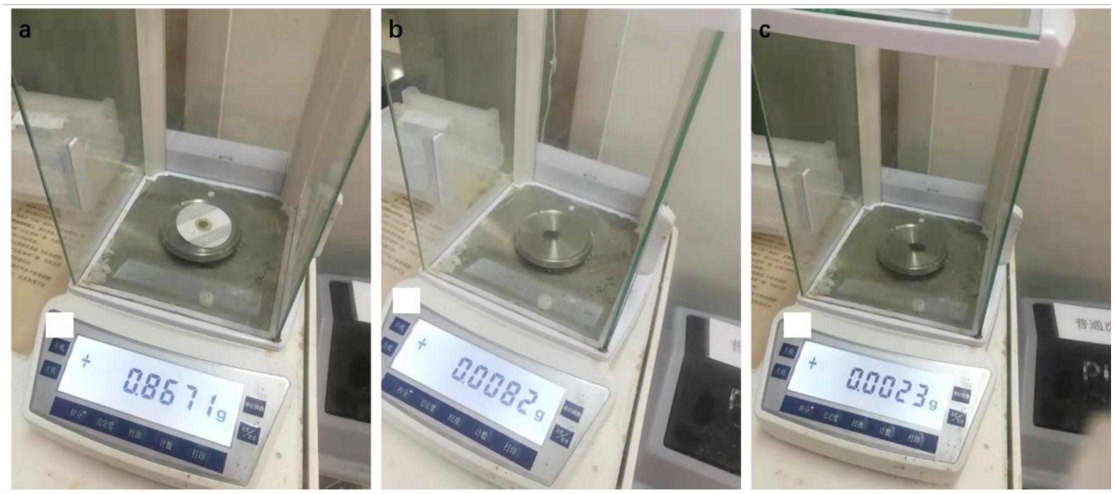

Fig. S9. The weight of (a) the Commercial gel electrodes (867.1 mg), (b) the LSG electronic skin with substrate layer (8.2 mg), and (c) the SFG electronic skin (2.3 mg).

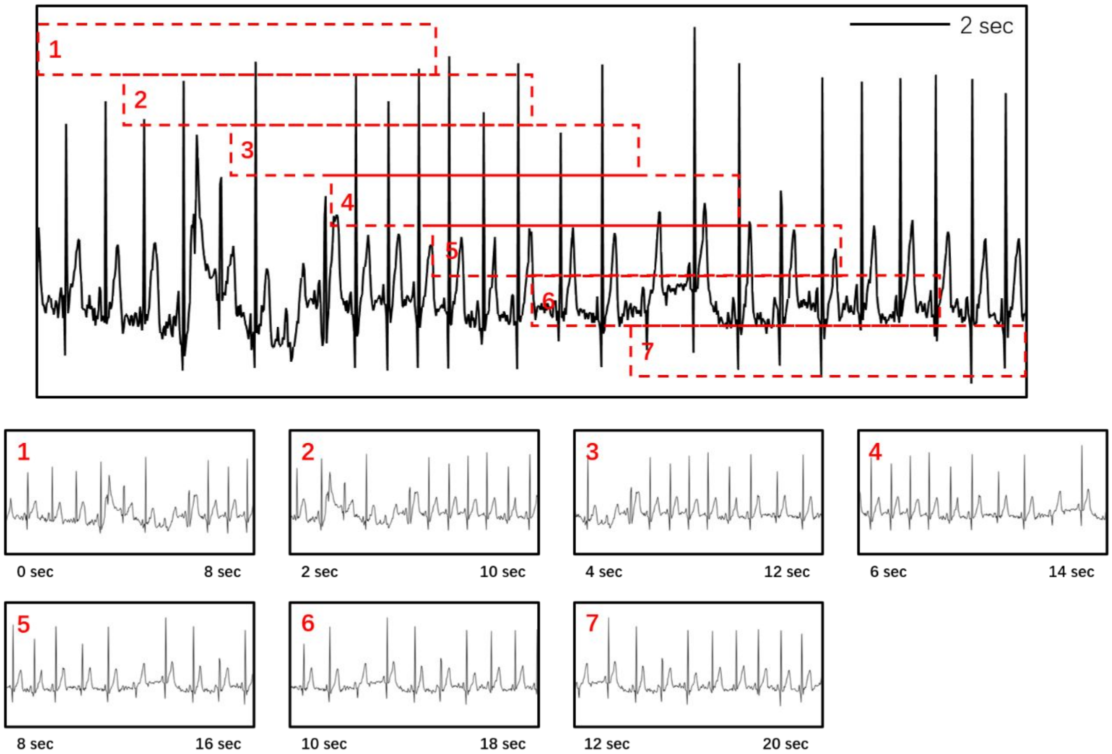

Fig. S10. Recognition of ECG signals by CNN. In order to increase the dataset and also to avoid the impact of improper segmentation of the ECG signal, the time interval between each segment is 2 seconds, in other words, the adjacent two segments have an overlap of 6 seconds. For example, a 20-second signal is split into 7 signals and each signal has a duration of 8 seconds. The first signal is from 0 to 8 sec and the second signal is from 2 to 10 sec. And so on.

Table. S1 Comparison between this LSG strain sensor and other graphene strain sensors.

Measuring Range	**GF**	**Reference**
100%	**316**	**This work**
8%	**518**	**This work**
14%	**102.8**	**This work**
5%	673	*ACS Nano*, **2018,** 12(9): 8839-8846.
10%	23	
280%	15	*Nat. Nanotechnol.* **2011,** *6*, 296-301.
35%	457	*Nanoscale* **2017,** *9*, 8266-8273
100%	268	
7.50%	400	*Nanoscale* **2016,** *8*, 20090-20095
0.62%	536.6	*Adv. Funct. Mater.* **2015,** *25*, 2395-2401
50%	522.6	*ACS Appl. Mater. Interfaces* **2016,** *8*, 5618-5626
140%	64	*Adv. Funct. Mater.* **2017,** *27*, 1604795.
100%	<8	*Adv. Mater.* **2014,** *26* , 2022-2027
1.60%	546	*ACS Nano* **2015,** *9*, 1622-1629.
4.50%	151	*Appl. Phys. Lett.* **2011,** *99*, 213107
410%	12.1	*Sci. Rep.* **2015,** *5*, 15554-15561.
500%	37.5	*Adv. Mater.* **2016,** *28*, 6640-6648
2%	1037	*Adv. Funct. Mater.* **2016,** *26*, 1322-1329
100%	10	*Adv. Mater.* **2015,** *27*, 7365-7371
2%	261.2	*ACS Appl. Mater. Interfaces* **2016,** *8*, 22501-22505
82%	150	*ACS Nano* **2016,** *10*, 7901-7906
1.50%	40	*Adv. Funct. Mater.*, **2018**, 28(52): 1805271.
20%	0.36	*Adv. Funct. Mater.*, **2016**, 26(13): 2078-2084.
70%	29	*Adv. Funct. Mater.,* **2015**, 25(27): 4228-4236.
86%	250	*ACS Appl. Mater. Interfaces,* **2018**, 10(50): 44173-44182.

Simulation of GSS

The COMSOL Multiphysics software is used to perform a two-fold modeling. Firstly, AC/DC model is applied on graphene acoustic devices with substrate of different materials, PMMA, Silicon chip, PVC and EP. The equation for joule heat model is

$$P = I\,V,\ \text{or}\ \frac{dP}{dV} = J \cdot E \quad (1)$$

Together coupled with COMSOL heat transfer interface, we modeled heat transferring from thermal acoustic device to the air. This is explained in CH.3 of the COMSOL heat transfer module user guide [1]. The properties of the materials such as their thermal conductivities can be found in the COMSOL material library [2].

Secondly, CFD and pressure acoustic model are applied on the surrounding air.

COMSOL Multiphysics analyzes the magnitude of acoustic output by solving the Helmholtz equation under frequency domain:

$$\nabla\left(-\frac{1}{\rho_c}(\nabla p_t - q_d)\right) - \frac{k_{eq}^2 p_t}{\rho_c} = Q_m \quad (2)$$

Where ρ_c is the density, p_t is total pressure q_d is dipole domain source, Q_m is monopole domain source. This is explained in Ch.2 of the COMSOL acoustic module user's guide [3].

In this case, we apply an AC potential of 5V, at frequency 1000Hz, across a 2-D thermal acoustic device of said materials. Heat transfer module is applied from device to the air, at room temperature and 1 atm pressure, the sound pressure level (SPL) at 1000Hz frequency domain across the environment is solve by the COMSOL acoustic module.

Reference

[1] Heat Transfer Interface User's Guide, pp. 60-70. COMSOL Multiphysics® v. 5.4. COMSOL AB, Stockholm, Sweden. 2018

[2] COMSOL Multiphysics v.5.4 Material library. https://www.comsol.com/material-library

[3] acoustic User's Guide, pp. 51, pp238. COMSOL Multiphysics® v. 5.4. COMSOL AB, Stockholm, Sweden. 2018

Impedance and noise

In this work, the polymer between electrode and human skin is removed, as shown in Fig. 6c. In this way, the contact impedance between electrode and human skin can be significantly reduced, providing two benefits for the biological signal detection. (I) Thermal noise $\overline{v_n^2} = 4kTBR$ (R is resistance) contributed by the contact layer is reduced, thereby offering higher signal noise ratio (SNR) for the biological signal. (II) The reduced contact impedance leads to a low Z_{AB}. If a biological signal causes a impedance variation ΔZ_b, the impedance variation ratio of the overall system is presented as $\eta = \frac{\Delta Z_b}{Z_{AB}}$. Obviously, η becomes higher with a lower Z_{AB}. Thus, the system becomes more sensitive to the detection of biological signal.

Details of the CNN

The CNN-based prediction model is shown in Fig 6.a, which includes 9 layers convolution neural networks (CNN). The first part includes a CNN layer, a batch normalization (BN) layer, ReLU activation function, one CNN layer and a Maxpooling layer. The second part is repeated seven times, each part includes a CNN layer, ReLU activation function, one dropout layer, a CNN layer and a Maxpooling layer. After processed by the BN layer and ReLU function, the output is a 2D matrix. To achieve classification, a flatten layer is applied to transfer the 2D matrix to the 1D matrix. Following a dense layer, the output is processed by the SoftMax function to achieve the classification.

During the training of the model, due to the difficulty of collecting abnormal ECG data, we use MIT-BIH dataset as training dataset, validation dataset and testing datasets. In each epoch, the model will automatically update the parameters in the model based on the hyperparameters and the error between the predicted value and the ground truth. The parameters in the model are used to do feature extraction. Machine learning technology and CNN algorithm help us to mine the deeper features of different types of arrhythmias. Due to insufficient dataset and missing information at the beginning and end of the data after splitting the data, we collect data with a duration of 8 secs, and the interval between each two data is 2 secs, in other words, there is 75% overlap between two consecutive data.